

High-Calcium Fly Ashes of Selective Sampling and Products of Their Aerodynamic Separation

Olga M. Sharonova¹, Vladimir V. Yumashev¹, Natalia A. Oreshkina², Leonid A. Solovyov¹ and Alexander G. Anshits^{1,2}

¹Institute of Chemistry and Chemical Technology, Siberian Branch, Russian Academy of Sciences, ul. Karla Marksa 42, Krasnoyarsk, 660049 Russia

²Siberian Federal University, Svobodny pr. 79, Krasnoyarsk, 660041 Russia

KEYWORDS: coal fly ash, selective sampling, composition, dispersity, aerodynamic separation

ABSTRACT

The investigation has been conducted on high calcium fly ash products selectively sampled at five points in the ash collecting system (a fore-hearth and fields 1–4 of electrostatic precipitators (EPs)) of the facilities for pulverized burning of two brown coals of B2 (sub C) rank in boiler units with bottom ash removal and slag-tap removal.

Differences between the densities, the granulometric compositions, the contents of carbon particles in ashes of the fore-hearths, the chemical and phase compositions for ashes of fields 1–4 were identified, and the alteration regularities of the parameters depending on the sampling point were determined for each of the ash collecting facilities.

Analysis of equilibrium phase formation was conducted on a ternary diagram for CaO-Al₂O₃-SiO₂ system and differences in the phase composition of ash products from different EPs fields for each ash collecting facility were identified.

Differences in the particle size distribution between ashes from different EPs fields and between the heavy, medium, and light fractions generated by aerodynamic separation of ashes from EPs fields 1 and 4 were demonstrated.

INTRODUCTION

Fly ashes sampled at certain points of an ash collecting system at a heat power plant are ash products with a more stable and reproducible composition compared with ashes from ash dumps. Selective sampling is used in the world practice for aluminosiliceous fly ashes as intermediate products for further separation by dispersiveness and for composition stabilization in order to use them in concretes, as filling agents of polymer products, and as components of road pavements.

In an ash collecting facility of a heat power plant, partial separation of fly ashes by size and density occurs. A reduction in the particle sizes of the ashes along the gas-dust stream is a general tendency, but the dispersivenesses of the ashes from different heat power plants can be very different, which is associated with the

fineness of coal pulverization, the presence of unburned carbon-mineral particles, and other factors. For instance, the content of the <63 μm fraction is 35–91% for fly ashes from EPs field 1 according to the data for different heat power plants¹, while the respective range for EPs field 3 in the same ashes is 60–98%. According to the data from paper², the average size of the ash particles reduces 7 times (from 28.1 μm to 3.8 μm) in the transition from field 1 to field 3 of EPs.

Changes occur in the mineral-phase composition. For instance, it was demonstrated for aluminosiliceous ashes sampled in different EPs fields² that the content of quartz reduces and the quantity of the glass phase increases from field 1 to field 3, while the content of Al_2O_3 in the glass phase increases and the content of SiO_2 reduces. An increase in the content of glass (from 85.8 up to 96.2%) was also observed by the authors of paper³ in fly ashes from six sampling points, as well as a tendency for a reduction in the content of ferrosphenel from field 1 to field 3 of EPs.

Thus, selective sampling of fly ashes at different points in ash collecting facility allows generating products with different composition; some of these products can be used in their unmodified state in the construction industry and in production of composite and binding materials. Aerodynamic separation allows generating additional fine and ultrafine fractions with desired densities and sizes from these products without destroying the ash microspheres, in order to use them in production of improved cements, concretes, high quality plastics, rubbers, road pavements, paints, and ceramics.

High calcium ashes have a wider chemical composition and a more complex and variable mineral-phase composition due to the formation of different calcium containing phases and a greater variety of glass-crystal microspheres⁴. It was shown that high calcium fly ashes from coals of the Kansk-Achinsk basin sampled at different points of the ash collecting system are considerably different in terms of the dispersiveness (an ultradisperse fraction (<10 μm) prevails in some of them), the contents of unburned particles, free calcium oxide, ferrosphenel, quartz, calcium aluminate, sulfate compounds, and vitrocrySTALLINE microspheres⁵.

The objective of this study was to comparatively examine semi-products of fly ashes sampled at 5 points of the ash collecting systems at two heat power plants that burn two different coals of B2 (sub C) rank from the Kansk-Achinsk basin at different temperature in boilers with bottom ash removal and slag-tap removal.

RESEARCH SUBJECTS AND METHODS

The research subjects were the products of selective sampling of fly ashes generated from pulverized burning of brown coals from the Kansk-Achinsk basin at two power plants where coal is burned in boiler units with bottom ash removal and slag-tap removal. The characteristics of the coals, the brands of the boiler units, the temperatures in the combustor, the sampling points, and the marking of the ash products are shown in Table 1⁵⁻⁷; it follows from it that B2 (sub C) coals are used, the coal is burned in a P-67 boiler unit with bottom ash removal at 1350–1420°C for fly ashes of the Bfa series, and in a BKZ-420 boiler unit with slag-tap removal at 1400–1500°C for the Kfa series. While the trapping efficiency is close (98–98.5%), the yields of fly ashes and slag are different.

Table 1.

Physical and chemical characteristics of brown coals of Kansk-Achinsk basin, data for boilers, ash collection and Bfa and Kfa series fly ash sampling points (W_t^r - moisture, Q_i^{daf} , V^{daf} – heat of combustion and volatile matter of fuel in the dry ash free basis, A^d – ash content of fuel in the dry basis)

№	Characteristics	Series	
		Bfa	Kfa
1	Power station	BSDPS-1	KCHP-2
2	Field	Berezovsk mine	Irsha-Borodino mine
3	Coal rank ²³ (group ²⁴)	B2 (sub C)	B2 (sub C)
4	W_t^r , %	33.0	32.5
5	Q_i^{daf} , MJ/kg	25.92	27.05
6	V^{daf} , %	48.0	47.5
7	A^d , %	7	6.5
8	Boiler	P-67	BKZ-420
9	Slag removal	bottom ash removal	slag-tap removal
10	Flame temperature, °C	1350-1420	1400-1500
11	Ash collection efficiency, %	98.5	>98
12	Fly ash proportion, %	≥95	65
13	Slag proportion, %	≤5	35
14	Fly ash sampling points	Fore-hearth (FH) and fields 1-4 of EPs	

Aerodynamic separation was carried out in a laboratory facility, whose flowchart is described in paper⁸. 10 cm³ of ashes per cycle of operation were loaded and blown off in an aerodynamic tunnel until the carryover of lighter particles arriving in the cyclone was terminated. The heavy product remained in the aerodynamic tunnel, the medium product accumulated in the lower portion of the cyclone, and the light product was collected on the filter installed at the outlet of the cyclone. An air flow provided by a compressor with a linear speed of 0.051 m/s was used when separating ashes. The number of cycles was 1–3; the yield of the products was determined for each cycle, and then identical products were mixed and averaged, and samples were collected for analysis.

The samples of fly ashes were collected and prepared for analysis in accordance with the national standards^{9,10}. The bulk density was determined using the measuring container method for three parallel measurements in accordance with GOST 16190-70¹¹, according to which the discrepancy between the determinations should not exceed 1.5 abs. % of the arithmetic mean. The granulometric composition of the fly ashes from the fore-hearths and EPs field 1 was determined by dry sieving of samples according to GOST 18318-94¹² in a VP-S/220 vibration facility equipped with a set of sieves with mesh sizes of 0.4, 0.2, 0.16, 0.1, 0.063, and 0.05 mm; the sum of the fractions should be ≥98% of the material taken for sieving. The macroelement composition and the loss on ignition (LOI) were determined using the chemical analysis methods according to GOST 5382-91¹³ with measurement errors depending on the content of the given component and being as follows: SiO₂, ±0.15% when its content is 5–18 wt. % to ±0.30% when its content is 25–40 wt. %; Al₂O₃, ±0.15% when its content is 3–7 wt. % to ±0.20% when its content is 7–20 wt.

%; Fe₂O₃, ±0.15% when its content is 3–10 wt. % and ±0.20% when its content is 10–25 wt. %; CaO, ±0.20% when its content is 10–40 wt. % and ±0.30% when its content is 40–70 wt. %; MgO, ±0.20% when its content is 1–6 wt. % and ±0.40% when its content is 6–25 wt. %; SO₃, ±0.10% when its content is 1–5 wt. % and ±0.20% when its content is 5–17 wt. %; TiO₂, Na₂O, and K₂O, ±0.04% to ±0.06%.

The particle size distribution was examined using a MicroTech 22 laser analyzer manufactured by Fritsch. An Axioscop-40 optical microscope (Carl Zeiss) equipped with a Canon color image digital video camera was used in order to examine the morphology of the ash particles. The quantitative phase composition was determined via X-ray phase analysis using a comprehensive Rietveld method¹⁴ and minimizing the derivative difference¹⁵. X-ray diagrams were made using a PANalytical X'Pert PRO diffractometer with a PIXcel detector and a secondary graphite monochromator. An X-ray tube with a copper anode was used under the conditions 50 kV/30 mA. The X-ray diagrams were made in reflection geometry utilizing the Bragg-Brentano focusing principle. Samples were prepared by fine grinding in an agate mortar.

RESULTS AND DISCUSSION

One of the technical characteristics of the dispersed material used in practice is bulk density, which is a complex parameter depending on the composition of the material, the shape of the particles, and the particle size distribution. As follows from the data on the bulk density of the ash products at 5 sampling points (Fig. 1), there is a steady tendency for a reduction in the density along the gas-dust stream for both series (from the fore-hearth to field 4 of EPs), within the range of 1.22 to 0.63 g/cm³ for the Bfa series and 1.77 to 1.18 g/cm³ for the Kfa series. Thus, the selectively sampled ashes of two coals are considerably different; moreover, considerable density variations are observed within each of the series of these ash products.

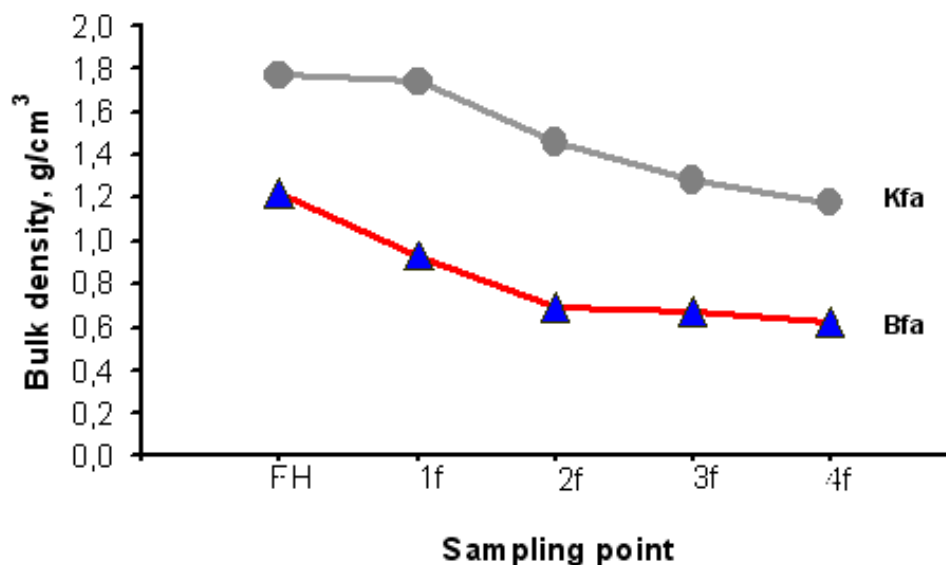


Fig.1. Bulk density (g/cm³) of fly ash products from five sampling points: fore-hearth (FH), fields 1-4 of electrostatic precipitators (1f-4f) for Bfa and Kfa series

The macrocomponent chemical composition of the examined ash products is shown as a diagram of chemical classification of fly ashes (Fig. 2) taken from paper¹⁶. Fly ashes from 46 heat power plants in Russia, Ukraine, and Kazakhstan^{1,17–20} were also plotted on the diagram, and it is clear that the overwhelming majority of them belong to the S (Sialic) type, ashes having a basic aluminosiliceous composition; a group of these ashes has an elevated Fe_2O_3 content ($>11.5\%$) and belongs to the FS (Ferrisialic) type. The examined ash products belong to the least studied high calcium ashes of the CS (Calsialic) and FCS (Ferricalsialic) types.

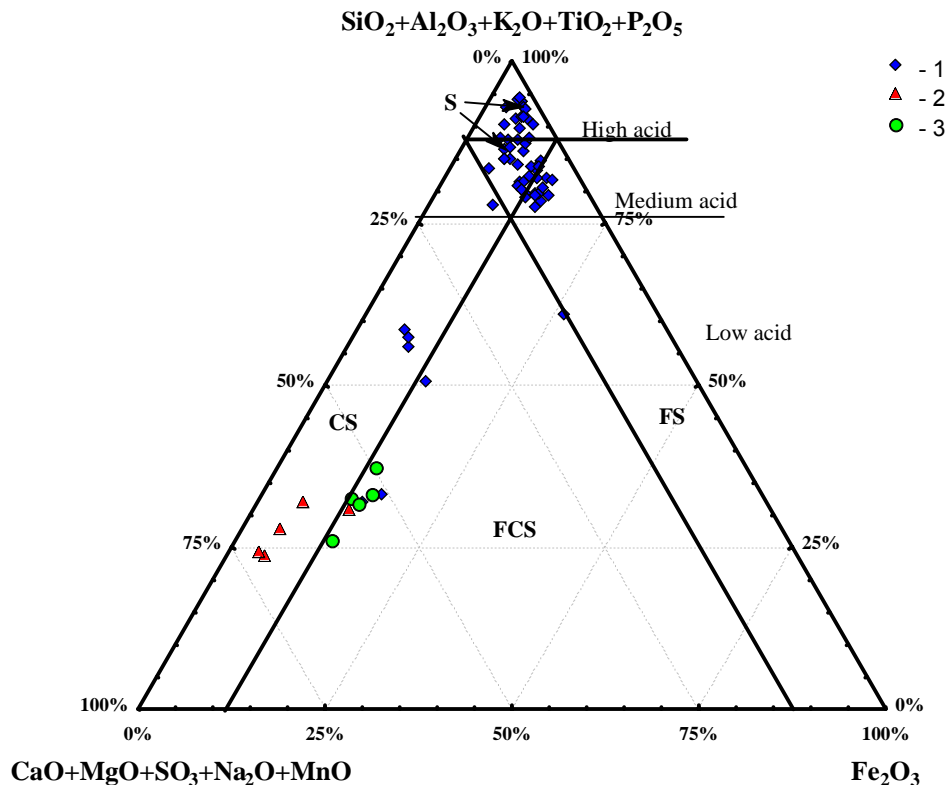


Fig. 2. Diagram of chemical classification¹⁹ of fly ashes with added composition of fly ashes:

- 1 – ashes of coal power plants of Russia, Ukraine and Kazakhstan^{20–23};
- 2 – ash products of Bfa series;
- 3 – ash products of Kfa series.

As follows from the data in Fig. 2, the principal specific feature of the Bfa series products from EPs fields 1–4 that belong to the Calsialic type is a low iron content (3.4–5.6 wt. % Fe_2O_3) compared with the products of the Kfa series (12.1–14.3 wt. % Fe_2O_3) that belong to the Ferricalsialic type. It should be noted that the Bfa series ash product from the fore-hearth with a Fe_2O_3 content of 11.1 wt. % also belongs to the Ferricalsialic type, which makes it considerably different from the other ashes of this series. As follows from Fig. 2, the compositions of the Bfa series products from EPs fields 1–4 are slightly different. This occurs primarily due to a reduction in the SiO_2 content (from 19.6 to 11.3 wt. %) and an increase in the SO_3 content (from 6.7

to 15.8 wt. %) in the transition from field 1 to field 4 of EPs. However, the differences in the composition of the Kfa series products from EPs fields 1–4 have a different nature: the SiO₂, SO₃, and MgO contents chaotically change, the Al₂O₃ content slightly increases, and the CaO content reduces. Thus, the behavior of fly ashes in ash collecting systems is different for coal burning in boilers with bottom ash removal and slag-tap removal.

While the compositions of the ash products from the fore-hearths of both series are quite close, the Bfa series product has a considerably lower density compared with the Kfa series. This fact can be explained by analysis of the data on granulometric composition (Fig. 3), which indicates that a higher yield of coarse fractions is observed in the case of the Bfa series, in particular, 0.2–0.4 mm and >0.4 mm fractions (12.6 and 15.7%, respectively). Determining the value of LOI (~25 and 32%, respectively) and the morphology of the particles using optical microscopy demonstrated that the particles contain many of unburned carbon particles that are porous lightweight particles, whose presence reduces considerably the bulk density of the Bfa series ash product from the fore-hearth. A distinctive feature of the Kfa series ashes from the fore-hearth is a low value of LOI (1.04%), and low contents of the 0.2–0.4 mm and >0.4 mm fractions (<3%), and therefore the content of carbon particles, which is a consequence of more efficient coal burning in the boiler unit with slag-tap removal at a higher temperature.

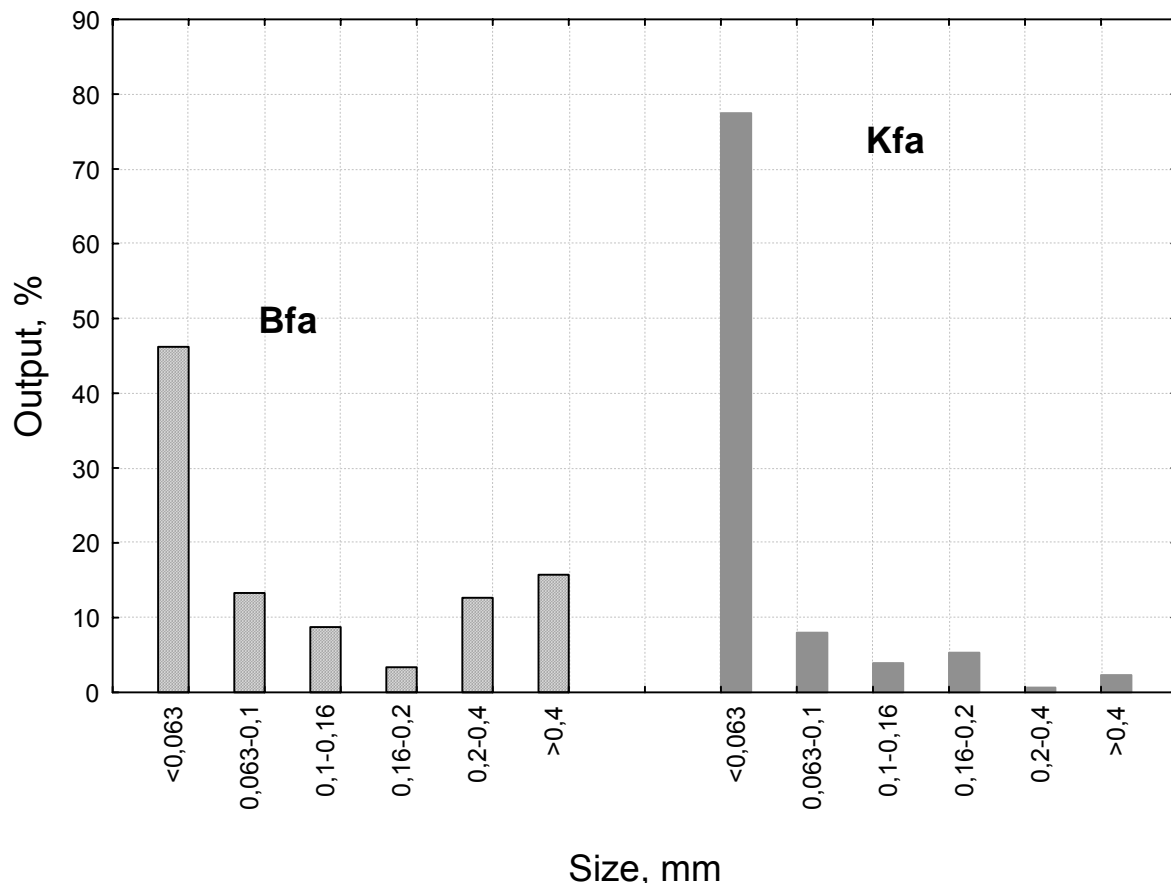


Fig. 3. Granulometric composition of ash products taken from fore-hearth for Bfa and Kfa series (LOI 14, 28 and 1.04 %, accordingly)

As was demonstrated previously when describing the data from the literature, using X-ray phase analysis for the products of selective sampling assists in more

effectively identifying the variation patterns of the product composition. The principal distinctive features of the phase composition of the Kfa series ash products from EPs fields 1–4 (Table 2) compared with those for the Bfa series are the presence of ferrosipinel, higher contents of calcium aluminate $\text{Ca}_3\text{Al}_2\text{O}_3$, calcium alumoferrite $\text{Ca}_2\text{Fe}_x\text{Al}_y\text{O}_5$, lime (CaO) and periclase (MgO) phases. Since these compounds have a higher crystallographic density compared with the other components of the phase composition, they make a considerable contribution to the density of these products. In addition, there are no hydrated phases having a low crystallographic density in the compounds.

Table 2.

Phase composition (wt.%) of Bfa and Kfa series fly ash products taken from fields 1-4 of EPs

Phase	Density,* g/cm ³	Fields 1-4 of EPs							
		Bfa series				Kfa series			
		1	2	3	4	1	2	3	4
Glass phase	-	23.6	28.0	26.9	33.6	19.0	28.6	32.6	33.1
$\text{Ca}_3\text{Al}_2\text{O}_3$	3.027	9.7	6.6	6.8	4.0	12.7	16.0	14.7	14.7
$\text{Ca}_2\text{Fe}_x\text{Al}_y\text{O}_5$	3.748	9.4	9.7	9.7	9.2	18.7	13.4	13.8	13.2
CaO	3.364	14.3	9.9	10.3	5.1	23.5	14.6	14.0	12.4
MgO	3.584	5.9	5.6	6.3	5.2	9.3	7.5	6.9	6.6
α - SiO_2	2.645	8.3	3.2	2.3	1.0	6.2	9.1	6.7	6.0
CaCO_3	2.702	6.3	5.7	8.7	7.8	-	3.9	3.0	2.9
CaSO_4	2.947	10.6	14.4	13.5	18.0	7.4	4.8	5.8	8.6
$\text{Al}_6\text{Ca}_4\text{O}_{12}\text{SO}_4$	2.606	2.1	3.0	2.6	2.7	-	-	-	-
$\text{Ca}(\text{OH})_2$	2.255	5.6	9.0	8.3	6.3	-	-	-	-
$\text{Ca}_6(\text{Al}(\text{OH})_6)_2(\text{SO}_4)_3 \cdot 0.5\text{H}_2\text{O}$	1.809	1.8	3.1	3.0	4.5	-	-	-	-
$\text{CaSO}_4 \cdot 0.5\text{H}_2\text{O}$	2.735	0.5	1.0	1.1	2.2	-	-	-	-
α - Fe_2O_3	5.274	1.7	0.8	0.6	0.3	-	-	-	-
Ferro-spinel	5.079	-	-	-	-	3.2	2.1	2.6	2.4

*Crystallographic density was calculated from ICSD (Inorganic Crystal Structure Database) structural data. $\text{Ca}_2\text{Fe}_x\text{Al}_y\text{O}_5$ density was calculated from $\text{Ca}_2\text{FeAlO}_5$ stoichiometry, ferro-spinel density was taken from magnetite.

Analysis of the changes in the phase composition of the Kfa series products from field 1 to field 4 of EPs indicates that there are steady tendencies for reducing the content of ferrosipinel 1.3 times, lime (CaO), 1.9 times, and periclase (MgO), 1.4 times; the content of the glass phase increases 1.7 times. The quantity of hematite (α - Fe_2O_3) in the Bfa series products reduces 5.6 times, calcium aluminate, 2.4 times, quartz (α - SiO_2), 8 times, and lime (CaO), 2.8 times. In addition, the content of anhydrite (CaSO_4) increases 1.7 times, the glass phase, 1.4 times, and hydrated forms $\text{Ca}_6(\text{Al}(\text{OH})_6)_2(\text{SO}_4)_3 \cdot 26\text{H}_2\text{O}$, 2.5 times, and $\text{CaSO}_4 \cdot 0.5\text{H}_2\text{O}$, 4.4 times.

Differences in the products of selective sampling are also quite noticeable on the phase diagram of CaO - Al_2O_3 - SiO_2 system taken from paper²¹ (Fig. 4). The Bfa series products from EPs fields 2–4 are the closest to Portland clinker; equilibrium phase formation will proceed in these products with hydraulically active clinker phases being generated (tricalcium silicate Ca_3SiO_5 , dicalcium silicate Ca_2SiO_4 , and calcium aluminate $\text{Ca}_3\text{Al}_2\text{O}_6$). The set of phases for EPs field 1 product will contain Ca_2SiO_4

and calcium aluminates $3\text{CaO}\cdot\text{Al}_2\text{O}_3$ and $12\text{CaO}\cdot 7\text{Al}_2\text{O}_3$. It should be noted that in the case of the slightest change in the composition of the product of field 1, the set of final phases will change, since the way of crystallization of the phases will shift toward the trisilicate calcium area or in the opposite direction, toward the gehlenite area. The Kfa series products from EPs fields 1–4 fall within the crystallization area of dicalcium silicate Ca_2SiO_4 . Crystallization of hydraulically active clinker phases (tricalcium silicate Ca_3SiO_5 , dicalcium silicate Ca_2SiO_4 , and calcium aluminate $\text{Ca}_3\text{Al}_2\text{O}_6$) is possible only for the composition of field 1, while in the case of fields 2–4, gehlenite $2\text{CaO}\cdot\text{Al}_2\text{O}_3\cdot\text{SiO}_2$ and rankinite $\text{Ca}_3\text{Si}_2\text{O}_4$ will be generated along with Ca_2SiO_4 , and the ratio between these phases will be different.

Although the composition points of the ash product are in the phase fields of dicalcium and tricalcium silicates (Fig. 4), the examined ashes do not contain these phases, while there is a considerable quantity of SiO_2 in the form of quartz, free CaO , and calcite CaCO_3 . The presence of free CaO is one of the principal factors constraining the application of ashes in their unmodified state in cement production. Therefore, targeted formation of the phases in the ash products promotes CaO binding, with hydraulically active phases of calcium trisilicates, calcium disilicates, and calcium aluminates being generated. In the presence of sulfate compounds in such high calcium ashes¹⁷, the interaction with CaO occurs at lower temperatures, with calcium disilicate being generated; the quantities of calcium sulfoaluminate and calcium aluminoferrite also increase. Depending on the temperature, calcium sulfosilicates can form, whose binding capacities depend on the composition and variety²².

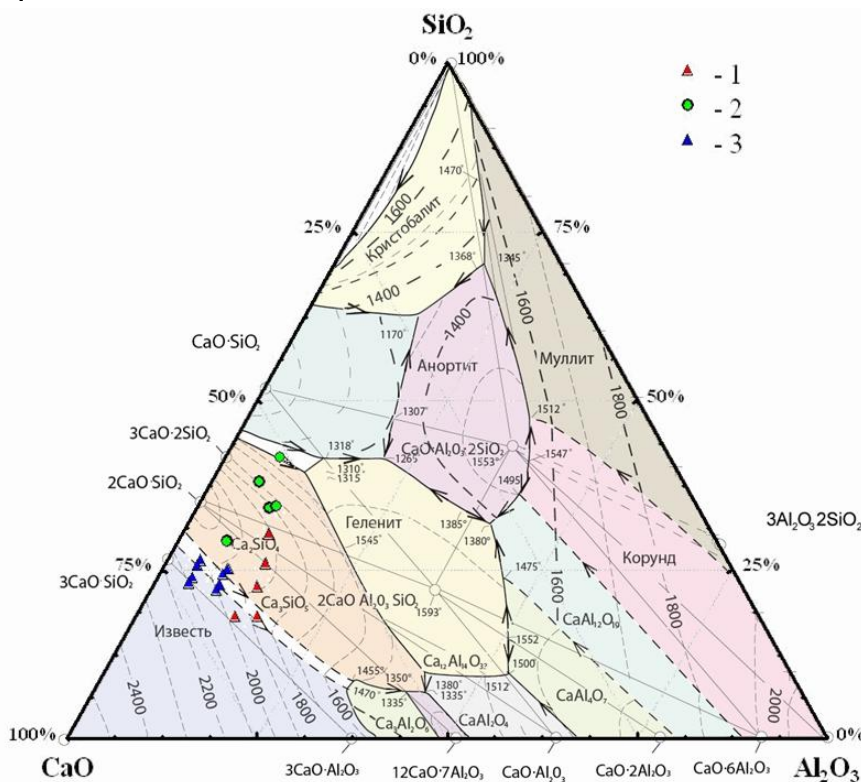


Fig. 4. Phase diagram of $\text{CaO}\text{-Al}_2\text{O}_3\text{-SiO}_2$ ²¹ with added compositions: 1 – ash products of Bfa series; 2 – ash products of Kfa series; 3 – Portland clinker²¹.

Thus, in order to use high calcium fly ashes in production of binding materials, dry ashes should be selectively sampled at different points of the ash collecting facilities at heat power plants. An additional treatment of the products of selective sampling allows performing targeted phase formation with a preset ratio between the hydraulically active phases, which in its turn allows increasing the contents of such products as cement additives to 30–50% without deterioration of their processing characteristics and using some of them as the main components of belite and belite-sulfoaluminate cements.

Differences in the particle sizes are observed (Fig. 5). As is seen, the particle size distribution for the Bfa series product from field 1 (its geometric mean diameter is 9.3 μm , and the d90 value is 42 μm) is considerably different from that for the ashes of fields 2–4, whose average diameters are 3.1, 2.8, and 2.4 μm , and the d90 value is 11.8, 9.1, and 7.9 μm , respectively. Another pattern is observed for the Kfa series, in which the products of fields 1 and 2 have close sizes (the geometric mean diameters are 11.7 and 12.3 μm , and the d90 value is ~ 40 μm), the product of field 3 is slightly different, and that of field 4 is quite different (the geometric mean diameters are 6.5 and 3.5 μm , and the d90 values are 30 and 12 μm , respectively). The particles of the Kfa series ash products from fields 1–4 have greater sizes compared with the Bfa series.

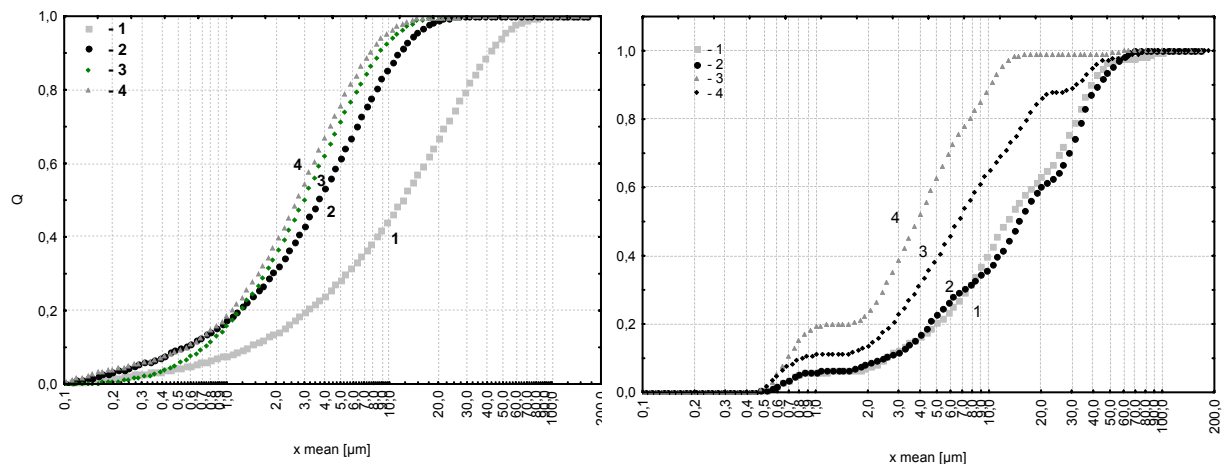


Fig. 5. Integral particles size distribution for ash products of Bfa series (left) and Kfa series (right) from fields 1-4 of electrostatic precipitators

The products of aerodynamic separation were examined. Analysis of the particle size distribution data indicates that separation of Bfa series fly ashes from field 1 proceeds quite efficiently, and the products have considerably different dispersivenesses (Fig. 6). In particular, the average diameter of the particles of the heavy product is 26.2 μm , while those of the medium and light products are 7.5 and 2.8 μm , respectively. An elevated Fe_2O_3 content is observed in the chemical composition of the heavy fraction, and the SO_3 and CaO contents and the value of LOI in the medium fraction are also elevated (Table 3).

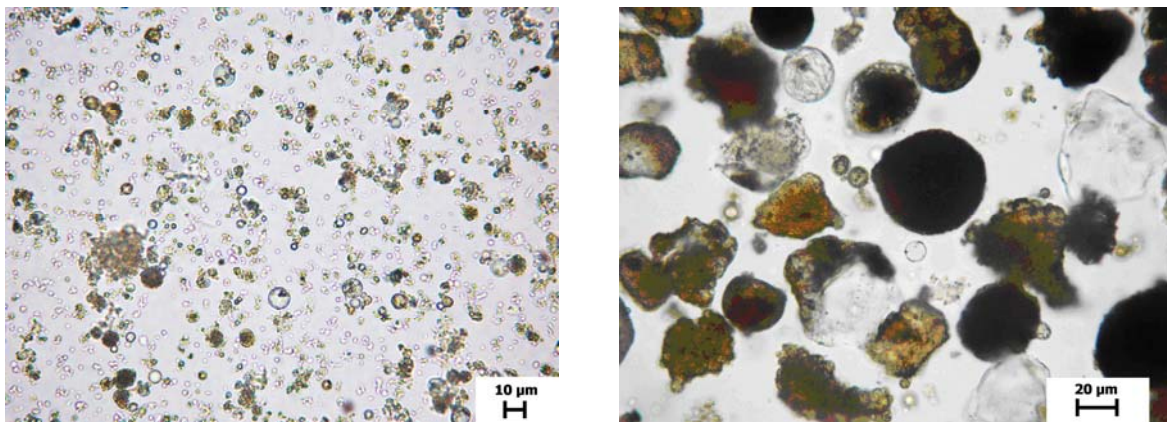
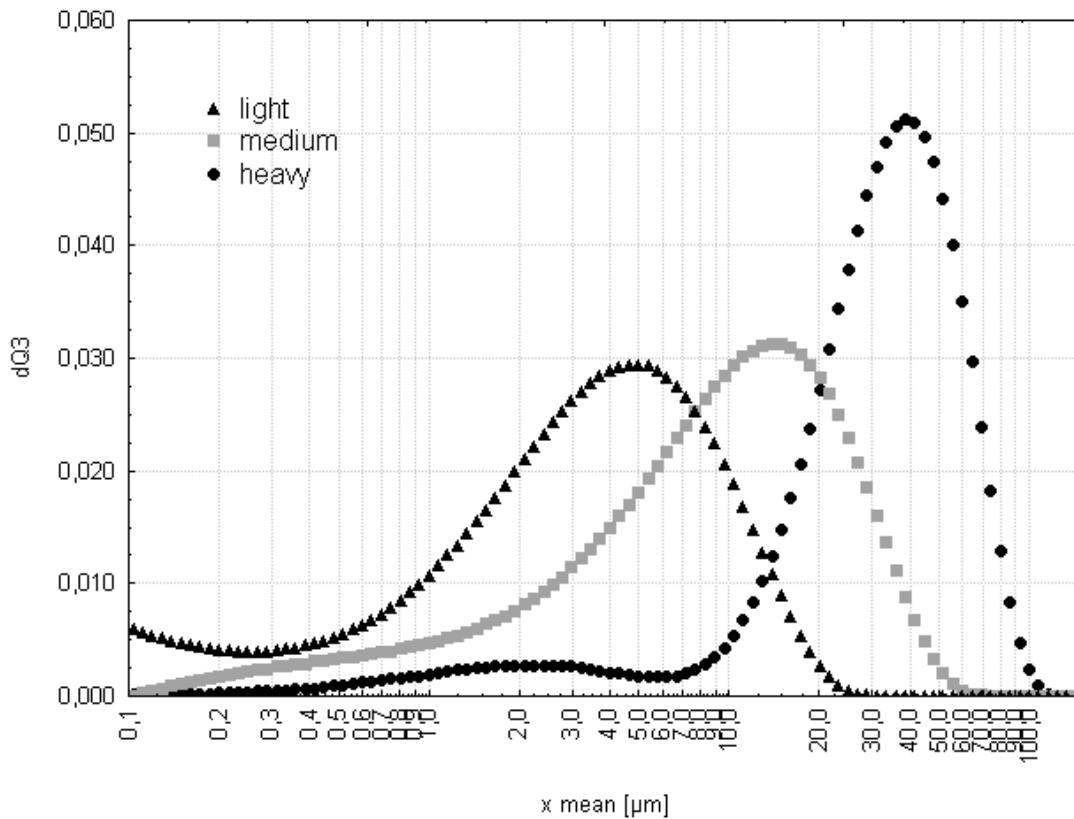


Fig. 6. Integral particle size distribution for products of the aerodynamic separation for fly ashes Bfa series from field 1 of electrostatic precipitators (at the top) and optical images of the light fraction (left) and heavy fraction (right)

A different conclusion follows from separation of Bfa series fly ashes from field 4. The size characteristics of the heavy and medium products are very close, while those of the light product change to a lesser degree compared with the ashes of field 1 (the average diameter of the particles is 4.8 to 2.9 µm). The ashes of field 4 are the most highly dispersed; their micron and submicron size particles are prone to aggregation, which reduces the efficiency of airflow separation of such particles (Table 3). In addition, such ashes without additional separation meet the requirements on the particles sizes for many applications. In the case of a wide particle distribution, which is typical for the Bfa series product of field 1 and for the

Kfa series product of fields 1 and 2, aerodynamic separation will be more efficient compared with the Bfa series of fields 2–4 and the Kfa series products of fields 3–4 .

Table 3.

Output (%), bulk density (g/cm³) and chemical composition (wt.%) of initial fly ashes of Bfa series taken from fields 1 and 4 of the electrostatic precipitators, and heavy and medium fractions of fly ashes aerodynamical separation

Data	Field 1			Field 4		
	initial	heavy fraction	medium fraction	initial	heavy fraction	medium fraction
Output	100	29- 33	52 - 56	100	53 - 62	23 - 31
Bulk density	0.93	1.13	0.79	0.63	0.72	0.59
SiO ₂	19.58	25.78	18.61	11.26	11.75	11.86
Al ₂ O ₃	9.86	9.98	9.48	9.87	8.99	8.57
Fe ₂ O ₃	5.62	7.17	4.55	3.39	4.48	3.37
CaO	45.88	42.80	46.27	41.21	38.43	41.01
MgO	4.36	4.88	3.98	4.50	4.60	4.81
Na ₂ O	0.79	0.39	0.56	1.91	1.56	1.46
K ₂ O	0.31	0.27	0.30	0.36	0.33	0.35
TiO ₂	0.13	0.89	0.15	0.06	0.32	0.58
SO ₃	6.67	3.38	7.34	15.78	14.56	14.61
LOI	6.30	3.98	8.28	11.20	14.34	13.12
Σ	99.51	99.51	99.50	99.54	99.40	99.39

Thus, the dispersiveness of the ash semi-products from the different fields of electrostatic precipitators is comparable to that of portland cements, and selective sampling allows changing purposefully the contribution of particles of different sizes within the range of 3 to 30 microns, which is very promising in cement production. Aerodynamic separation allows generating additional fine fractions with desired sizes and densities from these products.

CONCLUSIONS

The investigation has been conducted on high calcium fly ash products selectively sampled at five points in the ash collecting system (a fore-hearth and fields 1–4 of electrostatic precipitators (EPs)) of the facilities for pulverized burning of two brown coals of B2 (sub C) rank in boiler units with bottom ash removal and slag-tap removal (the Bfa and Kfa series, respectively).

It was demonstrated that the Bfa series fly ash from the fore-hearth contains >28% of coarse fractions (>0.2 mm) with a high content of unburned carbon particles unlike the Kfa series, in which the content of these fractions is less than 3%. The principal distinctive feature of the chemical composition of the Bfa series ash products from EPs fields 1–4 is lower Fe₂O₃ content and higher SO₃ content; consequently, their phase composition contains no ferrosphenel and considerably less calcium alumoferrite, but there is calcium sulfoaluminate and more calcium sulfate.

It was established that the bulk density reduces along the gas-dust stream for both series of the ash products. Steady reduction trends in the contents of phases of ferrosphenel, CaO, and MgO, and increase trend in the amorphous component are observed in the Kfa series. For the Bfa series, apart from CaO and MgO phases and the amorphous component, the quantities of hematite, calcium aluminate and quartz gradually reduce, and the quantities of anhydrite and hydrated forms increase.

Analysis of equilibrium phase formation was conducted on a ternary diagram for CaO-Al₂O₃-SiO₂ system and differences in the phase composition of ash products from different EPs fields for each ash collecting facility were identified.

It was demonstrated that the particle size distribution for the Bfa series ash product from field 1 is considerably different from fields 2–4 products. Another pattern is observed for the Kfa series, in which the particle sizes of the products from fields 1 and 2 are close, while the particle sizes of the products from fields 3 and 4 are different.

Aerodynamic separation of ash products from EPs field 1 and 4 was conducted, with the heavy, medium, and light fractions being generated, and it was demonstrated that it is most efficient for Bfa series ashes from EPs field 1.

REFERENCES

- [1] Panteleev V.G., Larina E.A., Melentiev V.A., Sergeeva T.E., Mokrushin A.R., Composition and characteristics of ashed and slag of heat power plants handbook. Leningrad: Energoatomizdat, 1985, p. 288 (in Russian).
- [2] Lee S.H., Kim K.D., Sakai E. and Daimon M. ,Journal of the Ceramic Society of Japan. 2003, 111, pp. 0011-0015
- [3] Shanthakumar S., Singh D.N., Phadke R.C., The 12 th International Conference of International Association for Computer Methods and Advances in Geomechanics (IACMAG), 1-6 October, 2008, pp. 2261-2267
- [4] Enders M. , Cement and Concrete Research. 1995, Vol.25, pp. 1369.
- [5] Sharonova O.M., Solovyov L.A., Oreshkina N.A., Yumashev V.V., Anshits A.G., Fuel Processing Technology, 2010, 91, pp. 573-581.
- [6] Vdovchenko V.S., Martynova M.I., Novitsky N.V., Yushina G.D.. Power fuel in the USSR: handbook. Moscow: Energoatomizdat, 1991, pp. 184 (in Russian).
- [7] Yeremin IV, Bronovets TM. Coal rank composition and rational utilization handbook. Moskow: Nedra; 1994, pp. 254 (in Russian).
- [8] Vereshchagin S.N., Kurteeva L.I., Anshits A.G., Chemistry for Sustainable Development , 2008, 16, pp. 529-536.
- [9] GOST 23148-98 (ISO 3954-77). Powders for powder metallurgy. Sampling. 1998. M., 1998, pp. 7.

- [10] GOST 26565-85. Unmoulded refractories. Methods of sampling and sample preparation. M., 1985. pp.13.
- [11] GOST 16190-70. Sorbents. Method of bulk density determination. 1970. M., 1970, pp. 4.
- [12] GOST 18318-94. Metallic powders. Determination of particle size by dry sieving. 1994, Minsk, 1994, pp. 7.
- [13] GOST 5382-91. Cement and materials for cement production. Chemistry analysis methods. 1991, M., 1991, pp. 94.
- [14] Rietveld M, J. Appl, Crystallogr. 1969, 2, pp. 65-71.
- [15] Solovyov L.A. , J. Appl, Crystallogr. 2004, 37, pp. 743-749.
- [16] Vassilev S., Vassileva C., Fuel, 2007, 86, pp. 1490-1512.
- [17] Ovcharenko G.I., Ashes coals of Kansk-Achinsk Fuel and Energy Complex in construction materials, Publishers Krasnoyarsk university , Krasnoyarsk, 1992, pp. 216. (in Russian).
- [18] Sharonova O.M., Anshits N.N., Orujeinikov A.I., Akimochkina G.V., Salanov A.N., Nizovski iA.I., Semenova O.N., Anshits A.G., Chemistry for Sustainable development, 2003, 11, P. 673.
- [19] Anshits A.G., Nizov V.A., Kondratenko E.V., Fomenko E.V., Anshits N.N., Kovalev A.M., Bajukov O.A., Sharonova O.M, Salanov A.N., Chemistry for sustainable development, 1999, 7, P.105.
- [20] Kizilshtein L.I., Dubov I.V., Shpitsgluz A.L., Parada S.P.. Components of ashes and slag of heat power plants. Moscow: Energoatomizdat; 1995. pp.176
- [21] Sheludyakov L.N., Kosanov Y.A., Marconrencov U.A., Complex processing silicate waste, Alma-Ata: Nauka, 1985, pp. 172 (in Russian).
- [22] Sherman N., Beretka J, Santoro L., Valentim G.L., Cement and Concrete Research, 1995, 25, pp.113-126.
- [23] GOST 25543-88. Brown coals, hard coals and anthracites. Classification according to genetic and technological parameters, 1988
- [24] ASTM D388-98a. Standard Classification of Coals by Rank, 1998